ALGORITHM FOR UPTAKE ASSESSMENT IN SMALL LESIONS BASED ON DYNAMIC SCINTIGRAPHY SCANS[*]

Milica M. Janković[1], Vera Miler Jerković[1], Ana Koljević Marković[2], Dejan B. Popović[1]

[1]University of Belgrade – Faculty of Electrical Engineering, Belgrade, Serbia
[2]National Cancer Research Center of Serbia, Belgrade, Serbia

Abstract. *The aim of our research was to develop an algorithm for estimation and visualisation of radiopharmaceutical uptake based on time-activity-curve (TAC) analysis in small regions of interest (ROI) in scintigraphic studies. The algorithm is implemented in Labview environment (National Instruments, Texas, Austin) and comprises the following steps: 1) delineation of grid of small ROIs over the examined tissue and corresponding TAC processing; 2) background vs tissue separation; 3) the extraction of all "suspected" ROIs where TACs are not exponentially descendent; 4) correlation analysis between a TAC corresponding to the central suspected ROI and TACs of neghboring ROIs; 5) the extraction of representative TAC for "suspected" area by Principal Component Analysis technique; and 6) visual interpretation of radiopharmaceutical distribution in the "suspected" area. The application of algorithm is presented in data recorded in case of histopathologically proven parathyroid tumors.*

Key words: *uptake, time activity curve, Principal Component Analysis, parathyroid tumor*

1. INTRODUCTION

Scintigraphy is a nuclear medicine diagnostic test for the visualization of spatial distribution of radioactivity uptake in a tissue. Radioactivity is taken by injection, inhalation or swallowing of medical agents (radiopharmaceuticals) with incorporated radioisotopes and the spatial distribution of radioactivity uptake is monitored by planar scintillation camera, SPECT (*Single Photon Emission Computer Tomography*) or PET (*Positron Emission Tomography*) camera.

Dynamic scintigraphy is a diagnostic test for examining the function of organs and physiological systems. The result of this type of scintigraphy is a series of frames (dynamic scintigrams) recorded in short time intervals (10 seconds to 1 minute apart, depending on the type of organ and disease). Time activity curve (TAC) is a quantitative indicator of

---

radioactivity uptake changes in a specific region of interest (ROI) over time. Distinguishing typical TAC patterns is of great importance for diagnostic purposes.

Beside the diagnostic application, scintigraphy has a very important place as a technique of preoperative imaging whose main goal is the precise localization of lesions in order to perform minimally invasive surgery [2-5]. In our previous work, we presented a *Submarine* method, based on TAC monitoring in small ROIs and finding abnormal TAC patterns corresponding to lesions [6]. *Submarine* method has proven useful for preoperative dynamic scintigraphic imaging of small lesions, especially in case of parathyroid imaging [6-8].

In this paper we introduce an algorithm that allows the precise uptake assessment in small lesions based on dynamic scintigrams and visual interpretation of uptake distribution in lesion area based on visualization of correlation matrix [1,8]. This algorithm is implemented as an additional tool in *Submarine* software.

2. METHODS AND MATERIALS

Typical TAC pattern of health tissue consists of three phases: increasing *vascular* phase (the radioactivity in the target ROI is rapidly growing), accumulation *uptake* phase (radioactivity is accumulated in the target ROI) and *washout* phase (phase of exponential radioactivity decrease in the target ROI), [9]. In the case of lesions, the atypical TAC pattern (prolonged retention of radiopharmaceutical in the target tissue or even a peak of radioactivity in *washout* phase) could be observed, Fig. 1.
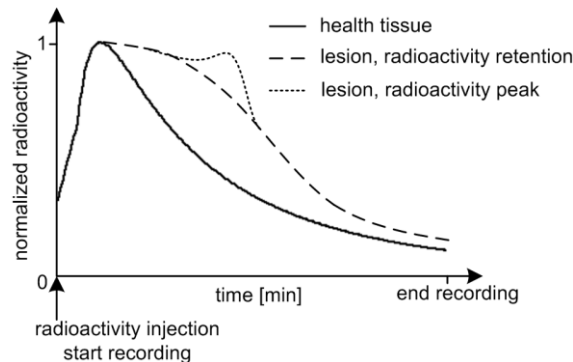
Fig. 1 Difference in TAC patterns for healthy tissue and lesion

In case of small lesions (<1 cm^3), it is very difficult or impossible to visually detect abnormal radioactivity uptake in individual frames, while it is clearly visible in the *washout* phase of TAC, Fig. 2.

Central ROI of lesion is delineated by black color in Fig. 2A, and another three ROIs shifted relative to the central ROI are also delineated. TACs corresponding to highlighted ROIs are presented in Fig. 2B (TAC_1, TAC_2, TAC_3, TAC_4). A high degree of correlation between curves TAC_1 and TAC_2 ($r=0.93$), TAC_1 and TAC_3 ($r=0.97$) could be observed, versus substantially less correlated TAC_1 i TAC_4 ($r=0.67$). TACs corresponding to regions positioned over the lesion are not exponential in *washout* phase and are strongly correlated. This fact is used for defining the algorithm for uptake assessment and its visualization in small lesions.
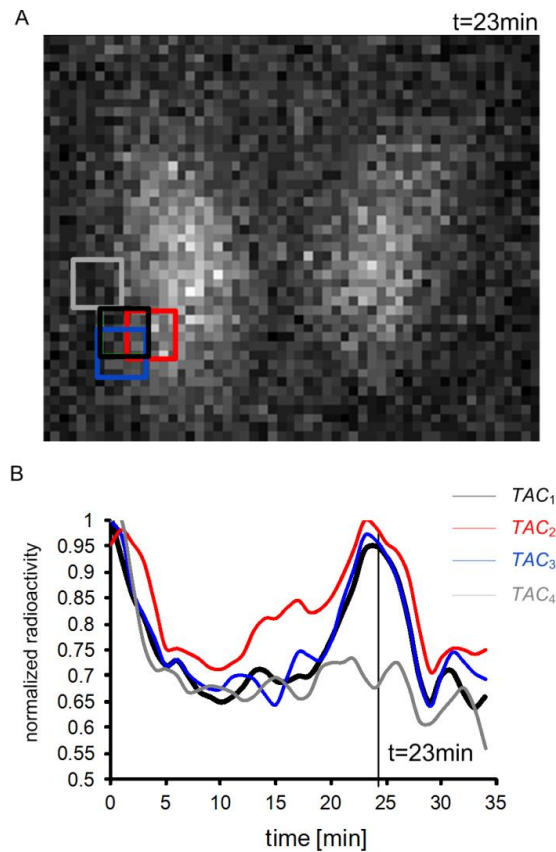
Fig. 2 A) A single frame from a dynamic image sequence, taken at the 23th minute,
with delineation of ROIs in the region of lesion (4×4 pixels, 6×6 mm)
B) TACs corresponding to ROIs delineated in A)

2.1. Software

The algorithm is implemented in the software for reading and processing dynamic studies introduced by authors in previous work [10]. Software is developed in Labview 8.6 environment (National Instruments, Texas, Austin) and additional NI Labview Biomedical Toolkit.

Realized application enables:

- Selection and readout of a dynamic scintigraphic study consisted of DICOM [11] images (each frame is archived as a separate .dcm file);
- Rectangular cropping of frames to the region that is to be processed further – selection cropping position is performed on selected frame with visual inspection of cropping position in all frames;
- Localization and visualization of small lesions by algorithm for uptake assessment presented in Section 1.2.

Checking *Principal Component Analysis* conditions (see Section 1.3) for examples presented in Section 2 was performed in RStudio, version 0.98.976.

2.2. Algorithm description

The algorithm for small lesion localization and visualization consists of six steps shown in Fig. 3.

STEP1	Delineation of grid of small square ROIs over the examined tissue and TAC processing
STEP2	Discrimination between tissue and background
STEP3	Extraction of all "suspected" ROIs - TACs are not exponentially descendent
STEP4	Correlation analysis between a TAC corresponding to the central suspected ROI and TACs of neghboring ROIs
STEP5	Extraction of representative TAC for "suspected" area by *Principal Component Analysis* technique
STEP6	Visual interpretation of radiopharmaceutical distribution in the "suspected" area

Fig. 3 Flowchart of the algorithm for the uptake assessment in small lesions.
ROI – region of interest, TAC – time activity curve

Step 1 Cropped area, containing the tissue that will be examined, is automatically divided into N small square ROIs, equal in size n x n, where n is a number of pixels (n=4 is a default value, but user can change it). This number of ROIs (N) will be reduced in Step 2 into the number of ROIs (T) which belongs to the tissue ($T{\leq}N$). The number of tissue ROIs (T) will be reduced in Step 3 into the number of ROIs (M) whose TACs are not exponentially descendent ($M{\leq}T$) and thereby indicate the abnormal radioactivity uptake and the potential lesion.

TACs corresponding to all N ROI cells are calculated and smoothed by cubic spline technique using Labview function *Cubic Spline Fit.vi* [12]. User can adjust the value (range [0,1]) of *balance parameter* (input parameter of cubic spline function) taking into consideration the requirement that the coefficient of determination (*R-square*) is greater than 80% (user sets minimum *balance parameter* for which *R-square>80%*). Labview function *Goodness of Fit.vi* is used for estimation of *R-square* value based on the raw TAC and the cubic spline filtered TAC.

Step 2 Maximum values of radioactivity $TAC^{CS}_{i\,max}$ are calculated for all TAC^{CS}_i (i=1, N). Reference value P for discriminating tissue from background is calculated according to the following equation:

$$P = \max(TAC^{CS}_{i\,max}), \quad i=1,N \tag{1}$$

Further analysis continues only for those T ROIs ($T \leq N$) that belong to the tissue, which means that satisfy the condition $TAC^{CS}_{i\,max} > m \cdot P$, $0 < m < 1$. Coefficient m is 0.8 at default, but user can change it.

Step 3 After background vs tissue separation, normalization of TACs for all selected ROI cells is performed. Normalization to maximum values $TAC^{CS}_{i\,max}$ ($i=1,T$) is used. The *washout* phase of each normalized TAC^{CSN}_i ($i=1,T$) is fitted by exponential function of the form Ae^{-kt} (A, k − constants, t − time variable). Labview function *Exponential Fit.vi* (*tolerance*=0.0001, *Bisquare* method) is used for fitting implementation. As well as in the Step 1, coefficient of determination (*R-square*) based on TAC^{CSN}_i and the exponentially fitted TAC^{CSN}_i is estimated ($i=1,T$). The criterion for selection of ROIs with non-exponential TAC pattern is defined as: *R-square* < 0.6 (0.6 is the empirically determined threshold). Next step is performed only for those M ROIs ($M \leq T$) that satisfy the non-exponential criterion.

Step 4 For each suspected ROI, a correlation matrix C_j is determined in the following form:

$$C_j = \begin{bmatrix} c_{-n\ -n} & \cdots & c_{+n\ -n} \\ \cdots & c_{0\,0} & \cdots \\ c_{-n\ +n} & \cdots & c_{+n\ +n} \end{bmatrix}, \quad c_{0\,0}=1,\ j=1,M \tag{2}$$

where c_{xy} is a *Spearman* correlation between a TAC^{CSN} of suspected ROI (central ROI in the origin (0,0), see Fig. 4) and TAC^{CSN} of neighboring ROIs (central ROI moved pixel by pixel in all directions, for x-pixels along the horizontal axis and y-pixels along the vertical axis, where x and y gets any integer value from the range $[-n,n]$, see Fig. 4). The maximum displacement in pixels of central ROI is equivalent to the pixel ROI length n, which means that most number of moved ROIs are overlapped with the central ROI. For example, in case of $n=4$ pixels, correlation matrix has $(2n+1)^2=81$ coefficients of correlation.

Step 5 For „suspected" area around each suspected ROI (see Fig. 4), the representative radioactivity uptake pattern is calculated using *Principal Component Analysis* (*PCA*) that transforms a set of correlated original variables into a set of uncorrelated new variables [13]. A subset of L ROIs ($L \leq M$), well correlated to the central suspected ROI, is selected according to the criterion $0.8 < c_{xy} < 0.9$ (see Section 1.3). Selected TAC^{CSN}_i ($i=1,L$) are input vectors in the following equation:

$$PC_1 = a_{1_1}TAC^{CSN}_1 + a_{1_2}TAC^{CSN}_2 + \ldots + a_{1L}TAC^{CSN}_L \tag{3}$$

where PC_1 is the first principal component (has the greatest variance and gives the shape for representative uptake TAC pattern) and coefficients a_{1p}, $0 < p < L$ are known as principal coefficients. The sum of squares of the coefficients is one, which means that the amount of total variance of all original TAC^{CSN}_i ($i=1,L$) is equal to the amount of total variance of all principal components.

Step 6 Correlation matrix C_j can be visually represented by assigning colors from standard palettes (e. g. *rainbow* or *grayscale* palette) to correlation coefficients. Moving away from the lesion, correlation coefficients decrease that can be visually displayed as the transition from light to dark colors. Visualization images presented in this paper are resampled to the 32×32 matrix by a standard bilinear interpolation method [14].
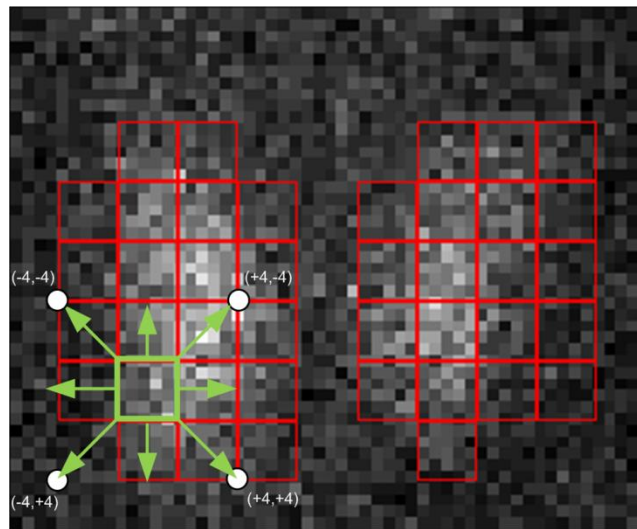
Fig. 4 An example of moving ROI (dimension 4×4 pixels, 6×6 mm) around the central suspected ROI (green color) when determining a correlation matrix. The suspected area is defined by arrows around the central suspected ROI. Other ROIs that belong to the tissue are presented by red color

2.3. *PCA* criteria

Preparation and pre-analysis *PCA* data are very important to demonstrate the validity of results. Analysis which need to be performed before running *PCA* are: 1) observing correlation matrix of selected TAC^{CSN}_i ($i=1,L$) and calculating the determinant; 2) the Kaiser-Meyer-Olkin (KMO) measure; 3) the Bartlett's test of sphericity.

Values in correlation matrix needn't be too low ($c_{xy}>0.8$), because the prerequisite for *PCA* is good correlation, or too high in order to avoid multicollinearity ($c_{xy}<0.9$) [13]. The value of determinant indicates on multicollinearity or singularity among original variables and it should not be less than 0.00001. In the case when the value of determinant is less than 0.00001, it means that some variables are highly correlated.

The Kaiser-Meyer-Olkin (KMO) is a measure of sampling adequacy [15]. It compares correlation and partial correlations between variables. KMO takes values between 0 and 1. The value of KMO should be greater than 0.5 if the sample is adequate. The Bartlett's test of sphericity is a test used to examine the null hypothesis: "Variables are uncorrelated, correlation matrix is an identity matrix". Therefore, we need to get *p*-value < 0.05 in this test and conclude that null hypothesis can be rejected.

For choosing the number of principal components we used the Kaiser rule and Screeplot combined with the amount of total variance that the chosen principal components have (the amount of total variance above 80 % is usually suggested) [16].

The rotation of principal components is used for improving interpretation of results. We have chosen the orthogonal rotation – varimax [16].

3. RESULTS AND DISCUSSION

We demonstrated the results of suggested algorithm for radioactivity uptake assessment in two patients who underwent parathyroid scintigraphy in the National Cancer Research Center of Serbia, Belgrade. Scintigraphic recording was performed in patients suspected of having primary hyperparathyroidism (PHPT) based on previous biochemical analysis (increased level of parathyroid hormone) and positive ultrasound findings. Patient data (biochemical, ultrasound, biopsy) are shown in Table 1.

Table 1 Patients: biochemical, ultrasound and biopsy data.
PHPT – primary hyperparathyroidism, PTH - parathyroid hormone

| Data	Patient 1	Patient 2
Gender	female	male
Age [years]	69	19
PTH [pg/ml]	223	125
PHPT ultrasound	positive	positive
Previous thyroidectomy	no	yes, right
Histopathology	parathyroid adenoma	parathyroid cancer
Tumor position	right inferior	left superior
Tumor volume [mm^3]	60	55

Siemens e.cam camera and Siemens Syngo e.soft 2007 software (Siemens AG, Erlangen, Germany) have been used for image acquisition. After intravenous ^{99m}Tc MIBI administration (with the radioactivity of 500 MBq, 13.5 mCi), 35 minutes of dynamic parathyroid scintigraphy (1 frame/min, dimension of image matrix: 128x128, pixel size 1.5 mm, zoom 3.2, anterior view) were performed.

Results of pre-analysis *PCA* data are presented in Table 2. All *PCA* criteria from Section 1.3 are satisfied (determinant value>0.00001, KMO>0.5, *p*-value<0.05 for Bartlett's test). First principal component carries more than 80% of total variance, which means that it is representative of TAC changes.

Fig. 5 shows results of algorithm applied in Patient 1 for two dimensions of ROI cells (3×3 pixels and 4×4 pixels). Visual inspection of standard dynamic scintigram at the moment of radioactivity peak in *washout* phase cannot distinguish lesion from healthy tissue, unlike suggested parametric imaging (Fig. 5A). Better discrimination between lesion and healthy tissue is evident in case of smaller ROI dimension, closer to the real lesion localization (compare Fig. 5A left and right). Representative TAC patterns are presented in Fig. 5B. The position of small parathyroid adenoma (right inferior) was surgically confirmed.

Table 2 Results of pre-analysis *PCA* data

Parameters	Patient 1		Patient 2
	3×3 pixels (4.5×4.5 mm)	4×4 pixels (6×6 mm)	4×4 pixels (6×6 mm)
Determinant value	0.00006	0.00009	0.00008
Kaiser-Meyer-Olkin value	0.855	0.806	0.805
Bartlett's test (*p*-value)	0.000	0.000	0.000
Number of principal components	1	1	1
Amount of total variance [%]	89.97	91.19	89.02
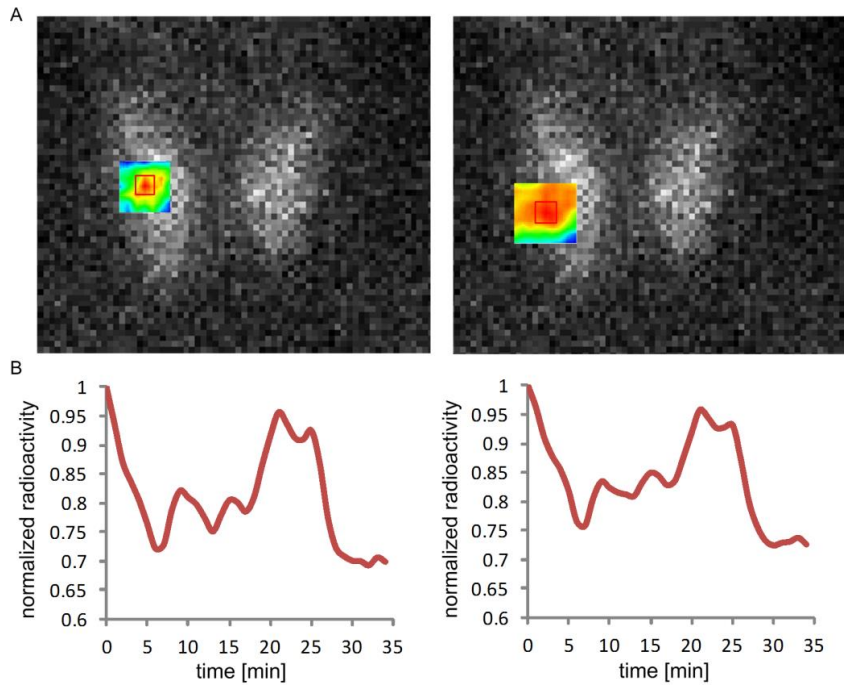
Fig. 5 A) A single frame from a dynamic image sequence, taken at the 22nd minute
and visual interpretation of lesion localization by introduced algorithm
B) Representative TAC patterns obtained by *Principal Component Analysis*

Fig. 6A shows results of visualization algorithm applied in Patient 2. Representative TAC pattern is presented in Fig. 6B. The position of small parathyroid cancer (left superior) was surgically confirmed.
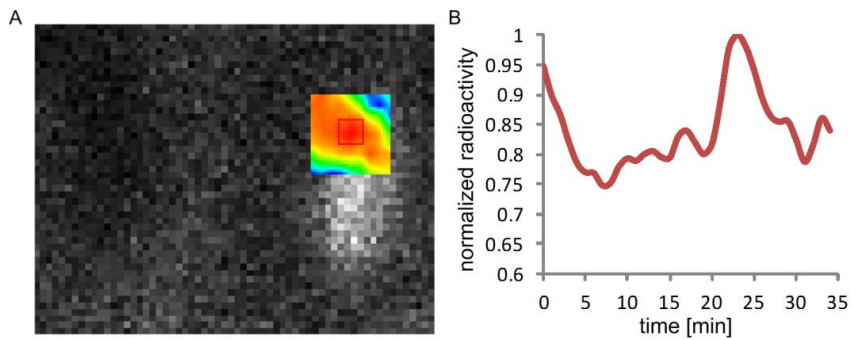
Fig. 6 A) A single frame from a dynamic image sequence, taken at the 24th minute
and a visual interpretation of lesion localization by suggested algorithm
B) Representative TAC pattern obtained by *Principal Component Analysis*

4. Conclusion

In this paper, we introduced an algorithm that enables the display of orientation, shape and boundaries of lesions. The algorithm visualizes the propagation of TAC correlation in the lesion area. The application of such algorithms is desirable in preoperative diagnostics in order to plan surgery. Further investigation will be related to the development of fully automated algorithm for lesion localization from dynamic scintigrams and its evaluation in a larger population with different oncological diseases.

References

[1] M. M. Janković, V. Miler Jerković, A. Koljević Marković and D. B. Popović, "Algorithm for the uptake assessment in small lesions in dynamic scintigraphy ", In Proceedings of the 58th ETRAN Conference, 2-5 June, Vrnjačka Banja, 2014, pp. ME 1.1 1-4 [In Serbian].

[2] D. Fuster, S. Vidal-Sicart, T. José-Vicente, P. Paredes, D. Rubello and F. Pons, "What is the role of preoperative scintigraphic imaging and the intraoperative gamma probe in secondary hyperparathyroidism?" *Nucl Med Commun*, vol. 35, no. 5, pp. 443-445, 2014.

[3] I. Stoffels, M. Müller, M.H. Geisel, J. Leyh, T. Pöppel, D. Schadendorf and J. Klode, "Cost-effectiveness of preoperative SPECT/CT combined with lymphoscintigraphy vs. lymphoscintigraphy for sentinel lymph node excision in patients with cutaneous malignant melanoma", *Eur J Nucl Med Mol*, [Epub ahead of print] 2014.

[4] M. Ibusuki, Y. Yamamoto, T. Kawasoe, S. Shiraishi, S. Tomiguchi, Y. Yamashita, Y. Honda, K. Iyama and H. Iwase, "Potential advantage of preoperative three-dimensional mapping of sentinel nodes in breast cancer by a hybrid single photon emission CT (SPECT)/CT system", *Surg Oncol*, vol. 19, no. 2, pp. 88-94, 2010.

[5] M. Giuliano, S.A. Gulec, D. Rubello, G. Boni, M. Puccini, M.R. Pelizzo, G. Manca, D. Casara, G. Sotti, P. Erba, D. Volterrani and A.E. Giuliano, "Preoperative localization and radioguided parathyroid surgery", *J Nucl Med*, vol. 44, no. 9, pp. 1443-1458, 2003.

[6] A. Koljević Marković, M. M. Janković, I. Marković, G. Pupić, R. Džodić and A. B. Delaloye, "Parathyroid dual tracer subtraction scintigraphy: small regions method for quantitative assessment of parathyroid adenoma uptake", *Ann Nucl Med*, vol. 28, pp. 736-745, 2014.

[7] M. Đurović M, M. M. Janković and A. Koljević Marković, " Semi-automatic localization of parathyroid tumors in dynamic sestamibi scintigrams ", In Proceedings of the 22nd Telecommunications forum TELFOR 2014, 25-27 November, Belgrade, 2014, pp. 955-958 [In Serbian].

[8] M. M. Janković, " Computer system for acquiring, storing, retrieving and processing images obtained by gamma camera ", PhD thesis, University of Belgrade – Faculty of Electrical Engineering, 2014 [In Serbian].

[9] M. P. Sandler, R. E. Coleman, J. A. Patton, F. J. Th. Wackers and A. Gottschalk, *Diagnostic Nuclear Medicine,* 4th ed. Philadelphia: Lippincott Williams & Wilkins, 2003.

[10] M. M. Janković, A. Koljević Marković and D. B. Popović, " Labview application for analysis of time activity curves in regions of small lesions in nuclear medicine ", In Proceedings of the 57th ETRAN Conference, 3-6 June, Zlatibor, 2013, pp. ME 1.9 1-5 [In Serbian].

[11] http://dicom.nema.org/

[12] J. S. Fleming and R. W. Kenny, "A comparison of techniques for the filtering of noise in the renogram, " *Phys Med Biol,* vol. 22, no. 2, pp. 359-364, Mar. 1977.

[13] J. E. Jackson and J. Wiley, *A user's guide to principal components*. New York: John Wiley and Sons, Inc., 1991.

[14] T. M. Lehmann, C. Gönner and K. Spitzer, "Interpolation Methods in Medical Image Processing, " *IEEE Trans Med Imag*, vol. 18, no. 11, pp. 1049-1075, Nov. 1999.

[15] H. F. Kaiser, "An index of factorial simplicity," *Psychometrika*, vol. 39, pp. 31-36, 1974.

[16] I. T. Jolliffe, *Principal Component Analysis*. 2nd ed. New York, USA: Springer, 2002.